

Mimicking human walking with 5-link model using HZD controller*

Maziar Ahmad Sharbafi¹ and Andre Seyfarth²

Abstract—Walking with 5-link model has been achieved by HZD (Hybrid Zero Dynamics) controller based on virtual constraints. These holonomic constraints are obtained by optimizing a set of virtual relations (e.g., Beziér polynomial) between system states which mostly do not have physical interpretations. In this paper, the virtual constraints are designed using human walking experiment data. Inspiring from human locomotion, different polynomials are extracted to mimic human joint angles patterns during walking. The virtual leg angle is the increasing variable which synchronizes the joints angles and defines the virtual constraints. Simulation results show that stable locomotion with leg and upper-body behavior similar to human experiment data is achieved for a wide range of speeds and body configuration parameters. VPP (Virtual Pivot Point) concept, a significant balancing feature found in human/animal locomotion, is investigated for different gait speeds as a performance index to compare the kinetic behavior of the simulated and human walking. Hence, we present human-like posture control as an outcome of motion control achieved by HZD with human inspired virtual constraints.

I. INTRODUCTION

Bipedal walking has been extensively investigated by researchers in the recent decades. Diverse control approaches were developed, from biologically inspired (e.g., CPG controllers [1], [2]) and conceptual model based approach (e.g., SLIP model [3], [4]) to engineering methods (e.g., ZMP [5] or HZD [6]). Most of the popular methods are focusing on one, either human locomotion or robot control technique. Applying the conceptual models as templates for control may be a useful approach to fill the gap between human experiments and robot control [7]. For this, abstraction is the key feature in simplifying the human locomotion problem, finding a solution and extending the simple control to the complex model, namely “template and anchor” [7]. Finding virtual pendulum concept in human/animal locomotion and utilizing it for postural control can be considered as another approach in extracting locomotion rules from nature and applying them to the machines [8]. The control rule resulted from this study is producing hip torque in order to redirect the ground reaction forces to a predefined Virtual Pivot Point (VPP). However, all control disciplines of human locomotion might not be as straight forward as this one. Therefore, we select a well established control method with sufficiently flexible degrees of freedom, design it based on human experiment data and investigate existence of VPP.

*This research was supported by the EU project BALANCE under Grant Agreement No. 601003.

¹M. A. Sharbafi is with Lauflabor Locomotion Lab, Technical University of Darmstadt, Germany sharbafi@sport.tu-darmstadt.de

²A. Seyfarth is with Lauflabor Locomotion Lab, Technical University of Darmstadt, Germany seyfarth@sport.tu-darmstadt.de

Hybrid Zero Dynamics (HZD), employing feedback linearization as a powerful nonlinear control approach, is founded on defining some relations between the system states, namely virtual constraints [6]. These relations are defined as holonomic constraints on robot’s configuration which are mostly computed mathematically, based on optimization approaches [9], [10], [11]. In [12], Ames presented a linear spring-mass-damper system characterized by human experimental data, called “canonical human walking functions”, to generate virtual constraints of the leg movement, based on hip position. In other studies (e.g., [13], [14], [15]) similar constraints, were considered for copying human kinematic behavior in a model and/or a robot even without upper body.

In this paper, we utilize data from human walking experiments to extract internal relations between joints’ angles and stance leg orientation which hold the configuration harmonized during the gaits. It is shown that with such virtual constraints, mimicking human kinematic and kinetic walking behaviors is achievable. In our previous studies, the relation between VPP and HZD was investigated by conceptual models for hopping and running [16], [17]. Here, a five link model with a rigid upper body and two segmented legs is used to implement a human-inspired HZD controller for walking (See Fig. 1). With the presented controller, VPP exists for all speed and its contribution in motion speed is also analyzed. Postural stability is one of significant achievements of this paper which was not addressed in the previous studies with similar HZD controller [12], [13], [14],[15]. In addition, we show that the proposed controller is also robust against body parameters’ variations which shows that control rules are fixed even for different structures (e.g. distribution of mass and inertia). In summary, the results show three significant outcomes: 1) The human inspired HZD controller can stabilize the walking at different speeds. 2) The kinematics (gait trajectories like joint angles) are similar to those obtained in human experiments 3) VPP exists which can be interpreted as an index for similarity to human walking kinetics.

II. METHODS

A. Simulation model

A 5-link model¹ is defined with five rigid segments, four active joints and one passive contact with the ground as shown in Fig. 1. This model is widely used for different

¹The simulation model is a modified version of 5-link model presented in http://web.eecs.umich.edu/~grizzle/westervelt_thesis/code/

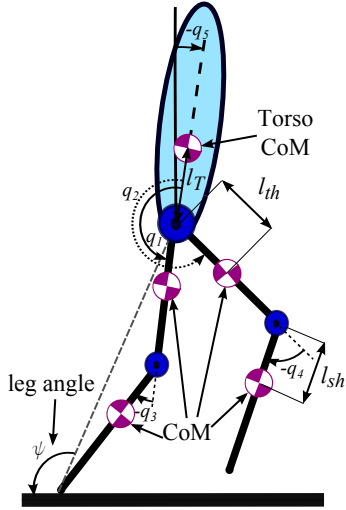


Fig. 1: The schematic of 5-link model.

TABLE I: 5-link model parameters with average weight and height from human experiments. The segments parameters are computed based on ratios in [18].

Name	Parameter	value	unit
M_T	Torso mass	47.9	kg
M_{th}	Thigh mass	7.1	
M_{sh}	Shank mass	4.4	
L_T	Torso length	0.81	m
L_{th}	Thigh length	0.46	
L_{sh}	Shank length	0.46	
l_T	Hip to torso CoM distance	0.3	m
l_{th}	Hip to thigh CoM distance	0.2	
l_{sh}	Knee to shank CoM distance	0.27	
I_T	Torso inertia	7.9	kgm^2
I_{th}	Thigh inertia	1.3	
I_{sh}	Shank inertia	0.7	
g	Gravitational acceleration	9.81	m/s^2
μ	Static friction coefficient	0.6	-

robots like Mabel [9] and Rabbit [19]. In our simulations, the model parameters are set to match the characteristics of a human with 70.9 kg weight and 1.73 m height (see Table I) which are the average values computed from the experiment subjects' body characteristics [20].

Walking dynamics (gait cycle) has two phases: *swing phase* (single support) and *stance phase* (double support). In single support, one leg (stance leg) is in contact with the ground when the other leg (swing leg) moves forward to complete the step. Based on the angles (q_i , $i = 1..5$) shown in Fig. 1, single support walking dynamics are defined using Lagrange equation on the angle vector $q = [q_1..q_5]^T$ as

$$D(q)\ddot{q} + C(q, \dot{q})\dot{q} + G(q) = Bu \quad (1)$$

in which D and C are the inertia and the Coriolis matrices, respectively. G is the gravity vector and B is a constant matrix that maps the joints' torques vector u to the generalized forces.

$$\dot{x} = \begin{bmatrix} \dot{q} \\ D^{-1}[-C\dot{q} - G] \end{bmatrix} + \begin{bmatrix} 0 \\ D^{-1}B \end{bmatrix} u = f(x) + g(x)u. \quad (2)$$

At the end of the swing phase, when the moving leg hits the ground (instant of touchdown) an impact occurs (instantaneous double support). With inelastic impact, the velocity of the contact leg end becomes zero instantaneously and the system initiates in a new continuous phase. Without impulsive actuation, integrating the system dynamic equation² over the impact duration results in $x^+ = \Delta(x^-)$, when superscript signs $-$ and $+$ describe the variables exactly before and after impact, respectively. Considering S as the manifold of double support configurations, the hybrid model will be

$$\Sigma = \begin{cases} \dot{x} = f(x) + g(x)u & x^- \notin S \\ x^+ = \Delta(x^-) & x^- \in S \end{cases} \quad (3)$$

B. Control approach

1) *HZD controller*: Hybrid zero dynamics (HZD) analysis and HZD controller based on virtual constraints were developed in [21] and [22]. HZD controller is selected in this paper for its outstanding stability analysis background and successful applications to different robots [23], [24], [10] and [11]. In HZD, holonomic constraints on the robot's configuration which are asymptotically achieved through the feedback control action are defined as virtual constraints by $y = h(q)$ [25]. In other words, virtual constraints' concept presents the ability to reproduce a desired kinematic behavior of a mechanical construction, via designing the controller instead of using the physical mechanism [6]. The control torque is determined via feedback linearization to regulate the output (y) to zero which should prepare a stable attractive manifold, namely "hybrid zero dynamics manifold". Since its stability cannot be evaluated in the stage of designing the output, some free parameters are considered in output definition to be used later to stabilize this manifold. The output only depends on the angles ($h(x) = h(q)$) and from the second order system (2), the system relative degree is 2 and the following controller results in the input-output linearization.

$$u(x) = (L_g L_f h(x))^{-1} \overbrace{(-K_D \dot{y} - K_P y - L_f^2 h(x))}^v \quad (4)$$

$L_f h(x) := \frac{\partial h}{\partial x} f$ is the Lie derivative of h along f and repeating this operator on $L_f h(x)$ along g and f , results in $L_g L_f h(x)$ and $L_f^2 h(x)$, respectively. We assume $L_g L_f h$ is invertible. Putting (4) in (2) results in $\ddot{y} = v$, a linear differential equation between the new input v and the output y which converges exponentially to zero employing a traditional *PD* controller. Thus, the input-output stability is gained; but the internal stability depends on the stability of the internal dynamics. On the zero dynamics manifold $Z := \{x | h(q) = L_f h(q) = 0\}$, the internal dynamics are simplified to the zero dynamics. The stability of the zero dynamics is investigated using Poincaré map analysis (see [6] for more details).

²At impact, to consider the external force at the end of the second leg, Eq. (2) is written with two more degrees of freedom (e.g., adding the second foot position to the generalized coordinate). For more details, see [6].

2) *Virtual Constraint from human experiment*: In order to define the virtual constraints, the outputs (of dimension 4) should be determined as functions of the angles and a monotonically increasing variable $\theta(q)$. Similar to [21], we select the first four angles $[q_1 \dots q_4]$ and also $\theta(q) := \psi$, the leg angle shown in Fig. 1, for output definition.

$$y = \begin{bmatrix} y_1 \\ y_2 \\ y_3 \\ y_4 \end{bmatrix} := \begin{bmatrix} q_1 \\ q_2 \\ q_3 \\ q_4 \end{bmatrix} - \begin{bmatrix} h_1(\psi) \\ h_2(\psi) \\ h_3(\psi) \\ h_4(\psi) \end{bmatrix} \quad (5)$$

where $h_i(\psi)$ is a function of the leg angle (for $i \in [1, 2, 3, 4]$). In [21], it is shown that with these output definition, virtual constraints can be found to simplify zero dynamics computations. The only remained step in designing the HZD controller is defining the desired evolution of the angles with appropriate functions $h_1(\psi)$ to $h_4(\psi)$. We extract these functions from experimental data by fitting a 5 degree polynomial of the leg angle to each joint angle q_i . It means that, we employ walking data to define the virtual constraints between the joint angles and the leg angle. This is the main difference of this paper with the previous studies which can reproduce the human walking patterns in a closed loop manner.

C. Experimental data

The data was collected in walking experiments on a treadmill (type ADAL-WR, Hef Tecmachine, Andrezieux Boutheon, France) at different speeds. Motion capture data (Qualisys, Gothenburg, Sweden) from 11 markers and ground reaction force data (12 piezo-electric force transducers within the treadmill) were collected. Twenty one subjects (11 female, 10 male) were asked to walk at different percentages of their preferred transition speed (PTS)³. The treadmill speed which equals the average velocity during strides was employed as the walking speed. The subjects were between 22 to 28 years old with $1.73 \pm 0.09m$ height and $70.9 \pm 11.7kg$ weight.

D. Finding VPP location

VPP (virtual pivot point) is a point where the ground reaction forces intersect in the coordinate system centered at CoM and with the body orientation as the vertical axis. This property, observed in human/animal locomotion [8], may be considered as a target for control or an index to evaluate the similarity of the control strategy to that of humans/animals. Thus, for every control approach, existence of the VPP which may convert the locomotion from inverted pendulum motion to a regular virtual pendulum (VP) can be investigated. VPP is defined in [8] as “the single point at which the total transferred angular momentum remains constant and the sum-of-squares difference to the original angular momentum over time is minimal, if the GRF is applied at exactly this point”. In this paper, the VPP is found using the calculations described in [26]. For every control approach, the existence

³PTS is the preferred speed for transition between running and walking which is typically about $1.9 - 2.1 m/s$ for humans [20].

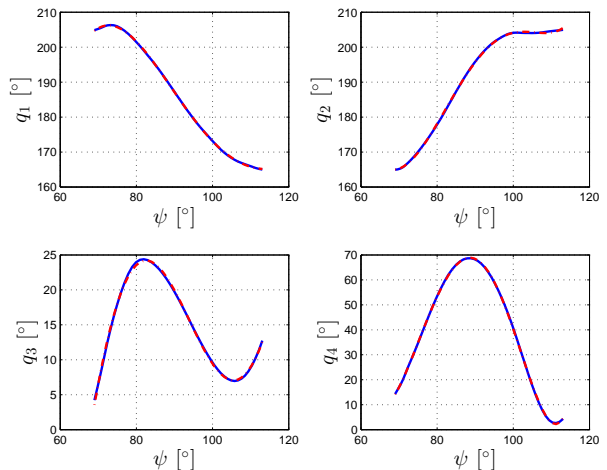


Fig. 2: The relation between the joint angles and the leg angle during one step. The blue line is the angles of the human experiment and the red dashed line is the 5 degree polynomial fitted to the data.

of a VPP is given when the ground reaction forces intersect at a point above the center of mass.

III. RESULTS AND DISCUSSION

In this section, a 5-link model is simulated based on the average values of human body parameters extracted from the walking experiment (see Table I). Similar to the experiments, 5 different gait speeds from 25%PTS to 125%PTS are simulated. As the preferred walking speed is about 75%PTS, first, we show the simulation results for this speed. The results and the design procedure are similar for the other speeds. Then, the human walking experiment results are compared to the simulated model for 5 different speeds. In that respect, existence of VPP and the relation between its position and gait speed are investigated. Finally, the same virtual constraints are utilized for different sets of body parameters to evaluate the robustness.

A. HZD controller design

In this section, we describe the HZD controller design and the results of walking with 75%PTS. The first step in designing the controller is defining the virtual constraints. We utilize the leg and joint angles (ψ and q_1 to q_4) mean values of 21 different subjects’ walking steps, as the references for computing the virtual constraints. As can be seen in Fig. 2, the joint angles are perfectly approximated with 5 degree polynomial functions of the leg angle. Unlike [12] which approximates the states as functions of time and then approximate time from hip position and velocity, we use the leg angle directly to coordinate the joints internally. Therefore, the joint angles can be synchronized by the leg angle which makes the controller time-invariant and robust against perturbation and parameter changes. Although these functions are extracted from human walking experiments with body characteristics presented in Table I, later, we

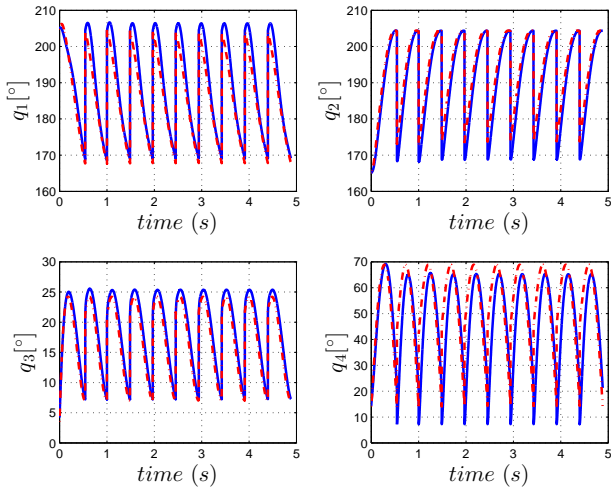


Fig. 3: Hip and knee angles of the swing and stance legs (defined in Fig. 1) during 10 walking steps with 75%PTS. Blue line shows the angles computed based on human inspired virtual constraints and red dashed line are the simulation responses with 5-link model.

apply the same virtual constraints for a different set of human body parameters and also for the parameters of Rabbit robot adopted from [6] and they work in both cases.

Since we do not optimize the virtual constraints to find an optimal controller with an attractive hybrid zero dynamics manifold, the resulted zero dynamics might not be hybrid invariant. To resolve this issue, we should check if a particular choice of parameters results in an exponentially stable walking cycle that is transversal to the switching surface S . Thus, it is needed to evaluate the restricted Poincaré map $\rho : S \cap Z \rightarrow S \cap Z$. Defining the vertical position of the swing foot by p_v^{sw} , the related Poincaré map should be checked on the following one dimensional surface

$$S \cap Z = \{(q, \dot{q}) | y = \dot{y} = 0, p_v^{sw} = 0\} \quad (6)$$

which gives 9 relations to compute the intersection of the zero dynamics manifold and switching surface. Therefore, considering ψ^- (the angular velocity of the stance leg before impact⁴), as the only remained unknown parameter, a one dimensional (local coordinate) representation of the Poincaré map can be computed as $\hat{\rho}(\psi^-)$. Finding initial value ψ^{*-} which satisfies $\hat{\rho}(\psi^{*-}) = \psi^{*-}$ gives the fixed point of the Poincaré map⁵. With 75%PTS, the asymptotically stable walking cycle is achieved with $\psi^- = 1.2 \text{ rad/s}$.

Employing appropriate *PD* coefficients in controller (4), results in tracking the desired joint angles, computed from virtual constraints, as shown in Fig. 3. The periodic motion

⁴Any joint angular velocity or combination of them can be selected. Here we chose ψ^- to have feeling about the motion speed.

⁵The procedure of computing the 1D Poincaré map $\hat{\rho}$ to check the existence and stability of the orbit is described for 3-segment model in Sec.6.6.1 of [6]. Here, the same method is applied to the 5-link model.

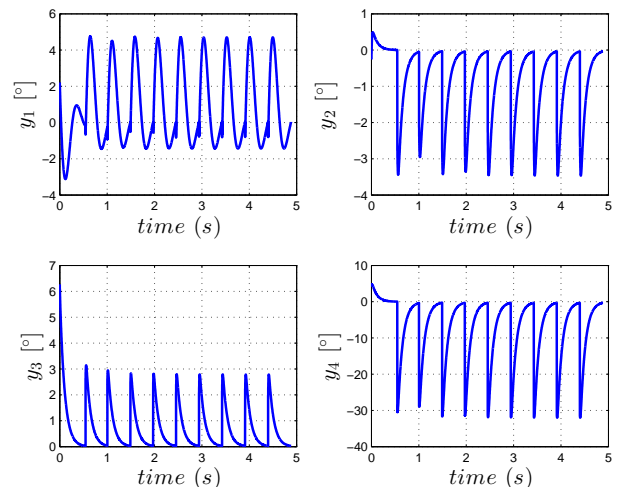


Fig. 4: The outputs (5), defined by virtual constraints as the difference between the joint angles and the 5 degree polynomial of the leg angle (deviations from zero dynamics), during 10 walking steps with 75%PTS.

as a result of converging to the stable limit cycle is depicted in this figure. Since the outputs are defined by differences between the angles and their desired values, they determine deviations from zero dynamics manifold in different directions (joint angles). Fig. 4 shows that the outputs which should converge to zero get their maxima after impacts and then vanish during swing phase. The output regulation (to zero) is sufficiently fast to return to zero dynamics manifold before the next impact. It means that though the zero dynamics is not hybrid invariant, it is attractive enough to cope with the errors caused by impact. Therefore, with the virtual constraints, generated based on human walking experiments, a stable gait with regular walking speed (75% PTS) is obtained. As explained before, the stability of the system is verified using the Poincaré map analysis of the zero dynamics which is a one order system. With this approach, after satisfying input-output stability of the system with feedback linearization (controller (4)), the eigenvalue of the Poincaré map of the zero dynamic system is checked. With eigenvalue inside the unit circle, the stability of the complete system (10th order system) is guaranteed.

B. Comparison with human experiments

In this section, the results of walking with HZD controller based on human experiment inspired virtual constraints are compared to experimental data for 5 different speeds. For each speed, we utilize the related experiment to extract an appropriate set of virtual constraints defined by four polynomials of degree 5. This virtual constraints identification stage finally gives 20 polynomials of degree 5. Then, for each gait we employ the related virtual constraints to generate the stable movement. Fig. 5 displays the leg, hip and knee angles of the experiments and simulations during one gait cycle. It starts with the values for the stance leg and after 50% of the gait cycle the angles relate to the swinging leg.

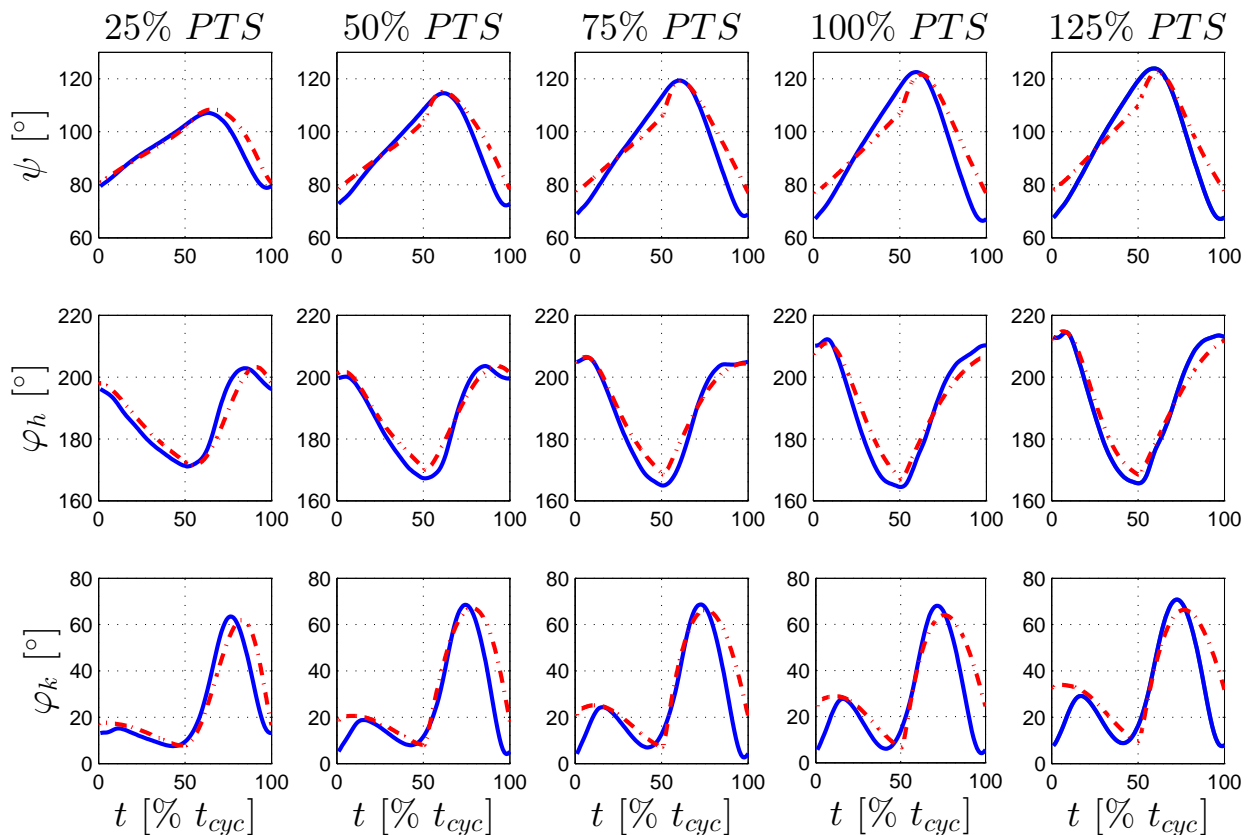


Fig. 5: The leg, knee and hip angles (ψ , ϕ_k and ϕ_h) of one gait cycle for different speeds. The blue line is the human experiment and the red dashed line is the simulation response with the 5-link model.

It is observed that the general trends of the experiment and simulation are similar for all gait speeds, especially for hip angle. The differences at the beginning and end of each step may come from modeling simplifications which consider instantaneous double support. The main important point is presenting a template for defining the virtual constraints based on human experiments which can stabilize the gait with similar movement patterns.

In order to investigate the kinetic behavior of the produced stable walking, we analyze the ground reaction force (GRF) and also employ the Virtual Pendulum (VP) concept as a feature in balancing the upper body. In Fig. 6, the GRFs directions are drawn with dashed lines from foot (center of pressure) when the coordinate system is centered at body CoM and the vertical axis shows the upper body direction. The VPPs computed for the simulation model and experiments (separately for each subject) are shown in this figure. As can be seen, the VPP exists in all gait speeds and the computed VPP points from simulations are in the neighborhood of the region found in human experiments, especially for walking faster than 25%PTS. Although with a fixed VPP, different gait speeds can be achieved [8], here, with a fixed controller architecture, changing the virtual constraints may be considered as a way of changing the VPP to adapt with the motion speed. However, balancing

(with VPP position) is not the only control mechanism for changing the speed. Another control layer also contributes to gait speed is leg adjustment which determines the step length and angle of attack and this contribution is sometimes more significant than postural control. Focusing more on Figs. 5 and 6 shows that for 75%PTS (regular walking speed) and more, in which the angle of attack is almost constant (about 77°) and the step length changes are smaller than that of the slower gaits, the effect of VPP position on motion speed is more visible. For these speeds, the further VPP from CoM, the longer virtual pendulum and equivalently, the larger upper body oscillations, required for the faster motion. It seems that for slow motions, the speed is controlled by swing leg adjustment and when balancing should be performed in a slower manner, longer pendulum length is needed and the VPP moved more upward. However, the existence of VPP during walking shows that the proposed controller tries to mimic the kinetic behavior of human walking, in addition to kinematics.

C. Robustness against model parameters

In order to investigate robustness of the proposed controller, we apply it to two other body structures (see table. II). The first parameter set corresponds to a human with 1.89 m height (with leg length 1 m) and 80 kg weight. The ratio

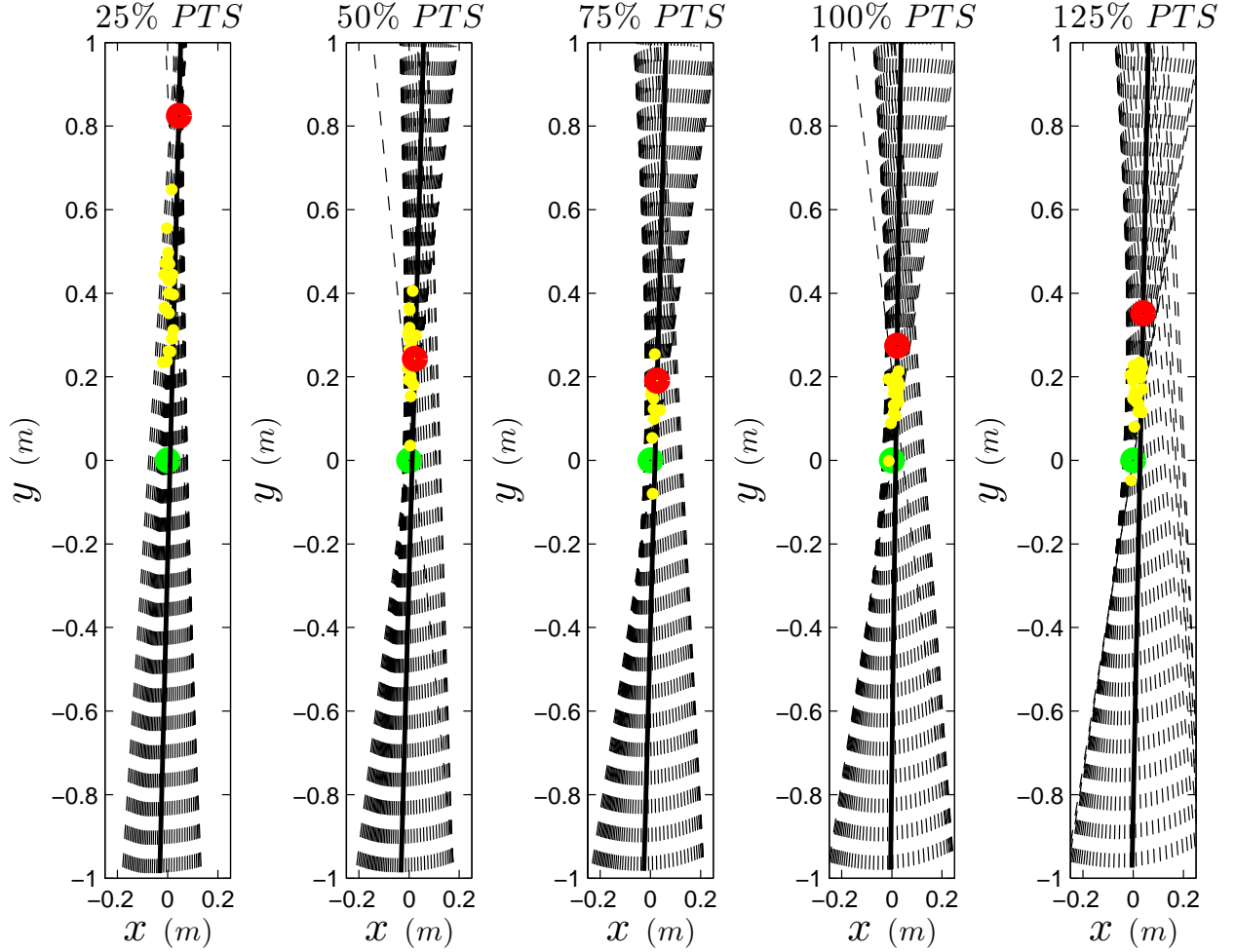


Fig. 6: Alignment of the GRFs (ground reaction forces) during one step. The VPP point and CoM are shown by red and green circles, respectively. Yellow circles are the VPPs found for different subjects from human experiments.

between different segments' masses, inertias lengths and CoM positions are similar to the average value of Table. I. The controller, proposed in the previous section, with the same parameters (virtual constraints and PD coefficients) is applied to the new body structure. It is noteworthy that a fixed controller works for different body characteristics. It shows that the virtual holonomic constraints are the basic rules of motion which should be considered to make stable walking and for each speed, irrelevant to body parameters, a specific set of virtual constraints is required.

Another example is the parameter configuration of the Rabbit robot [6]. Obviously, the structure and ratios of different segments' parameters are quite different to humans. Surprisingly, to stabilize the walking with this model, only the PD coefficients need to be adjusted. It means that with a fixed set of virtual constraints and only with tuning the convergence rate to the zero dynamics manifold which may be affected by the body parameters⁶, stable walking is

⁶The segments with different mass and inertias require different torques (equivalently different PD coefficients) to move similarly.

achievable. In other words, the basis of locomotion which is defined here with some relations between the states (synchronizing the joint angles variations using the leg angle) is determined for a specific motion with a diverse range of body characteristics.

TABLE II: 5-link model parameters with body characteristics of the Rabbit robot [6] and a sample human [18]

Parameter	RABBIT	human	unit
Torso mass	12	54	kg
Thigh mass	6.8	8	
Shank mass	3.2	5	
Torso length	0.63	0.89	m
Thigh length	0.4	0.5	
Shank length	0.4	0.5	
Hip to torso CoM distance	0.24	0.33	m
Hip to thigh CoM distance	0.11	0.21	
Knee to shank CoM distance	0.24	0.3	
Torso inertia	1.33	10.6	kgm^2
Thigh inertia	0.47	1.8	
Shank inertia	0.2	1	

IV. CONCLUSION

Compared to other approaches to stabilize the legged robot locomotion, here imposing some holonomic constraints between different body parts is the design key. Satisfying internal relation between the joint angles based on a unifying variable such as the leg angle is the way of implementing the proposed approach to control a 5-link model walking in this paper. However, if there exist some basic rules of control design that can be fixed even if the structure varies, the control design problem is converted to detect these rules. On the other hand, humans/animals body is a sample of intelligent, efficient and robust controller which can be investigated to find the rules. Therefore, our approach for finding these virtual constraints is employing human experiments. In that respect, the virtual relations between the joint angles and leg angles were developed based on experimental data. The controller satisfying these relations is able to stabilize walking in a wide range of body characteristics and speeds. It was shown that the controller for a robot (like Rabbit) can be obtained by satisfying the virtual constraints found in human gaits.

Another aspect in producing stable gait is mimicking humans' motion characteristics. It was also shown that with the proposed approach, in addition to similarity in kinematic behavior which was the first goal, the controlled model resembles some features of kinetic behavior of human gaits. The virtual pendulum property of human locomotion is a key feature in balancing exhibited by the HZD controller with human experiment inspired virtual constraints.

The results may suffer from inaccuracy in walking modeling like instantaneous double support. For example, one discrepancy from human locomotion is the effect of impact which can be seen as lack of swing leg retraction and jumps in speeds at touchdown moments. Completing the model to have a continuous double support and utilizing the derived control rules to empower the exoskeleton for stabilizing the motions with the least interference with human activities are the important future steps of this research.

REFERENCES

- [1] A. J. Ijspeert, "Central pattern generators for locomotion control in animals and robots: A review," *Neural Networks*, vol. 21, pp. 642–653, 2008.
- [2] D. Owaki, M. Koyama, S. Yamaguchi, S. Kubo, and A. Ishiguro, "A 2-d passive-dynamic-running biped with elastic elements," *IEEE Transactions on Robotics*, vol. 27, no. 1, pp. 156–162, 2011.
- [3] A. Seyfarth, H. Geyer, M. Guenther, and R. Blickhan, "A movement criterion for running," *Journal of Biomechanics*, vol. 35, no. 5, pp. 649–655, 2002.
- [4] H. Geyer, A. Seyfarth, and R. Blickhan, "Positive force feedback in bouncing gaits?" *Proceedings of the Royal Society B*, vol. 270, 2003.
- [5] M. Vukobratovic and Y. Stepanenko, "On the stability of anthropomorphic systems," *Mathematical Biosciences*, vol. 15, pp. 1–37, 1972.
- [6] E. R. Westervelt, J. W. Grizzle, C. Chevallereau, J. H. Choi, and B. Morris, *Feedback Control of Dynamic Bipedal Robot Locomotion*. Taylor & Francis, CRC Press, 2007.
- [7] R. J. Full and D. Koditschek, "Templates and anchors: Neuromechanical hypotheses of legged locomotion on land," *Journal of Experimental Biology*, vol. 22, pp. 3325–3332, 1999.
- [8] H. M. Maus, S. Lipfert, M. Gross, J. Rummel, and A. Seyfarth, "Upright human gait did not provide a major mechanical challenge for our ancestors," *Nature Communications*, vol. 1, no. 6, pp. 1–6, 2010.
- [9] K. Sreenath, H. Park, I. Poulakakis, and J. W. Grizzle, "A compliant hybrid zero dynamics controller for stable, efficient and fast bipedal walking on mabel," *International Journal of Robotics Research*, 2010.
- [10] B. Morris and J. W. Grizzle, "Hybrid invariant manifolds in systems with impulse effects with application to periodic locomotion in bipedal robots," *IEEE Transaction on Automatic Control*, vol. 54, no. 8, pp. 1751–1764, 2009.
- [11] I. Poulakakis and J. W. Grizzle, "The spring loaded inverted pendulum as the hybrid zero dynamics of an asymmetric hopper," *IEEE Transaction on Automatic Control*, vol. 54, no. 8, pp. 1779–1793, 2009.
- [12] A. D. Ames, "First steps toward automatically generating bipedal robotic walking from human data," *Lecture Notes in Control and Information Sciences*, vol. 422, pp. 89–116, 2012.
- [13] S. Jiang, S. Patrick, H. Zhao, and A. D. Ames, "Outputs of human walking for bipedal robotic controller design," in *American Control Conference (ACC)*, 2012.
- [14] M. J. Powel, H. Zhao, and A. D. Ames, "Primitives for human-inspired bipedal robotic locomotion: Walking and stair climbing," in *International Conference on Robotics and Automation (ICRA)*, 2012.
- [15] A. D. Ames, "First steps toward underactuated human-inspired bipedal robotic walking," in *International Conference on Robotics and Automation (ICRA)*, 2012.
- [16] M. A. Sharbafi, C. Maufroy, A. Seyfarth, M. J. Yazdanpanah, and M. N. Ahmadabadi, "Controllers for robust hopping with upright trunk based on the virtual pendulum concept," in *IEEE/RSJ International Conference on Intelligent Robots and Systems (IROS 2012)*, 2012.
- [17] M. A. Sharbafi, C. Maufroy, M. N. Ahmadabadi, M. J. Yazdanpanah, and A. Seyfarth, "Robust hopping based on virtual pendulum posture control," *Bioinspiration and Biomimetics*, vol. 8, no. 3, 2013.
- [18] D. A. Winter, *BioMechanics and motor control of human movement*, 3rd ed. New Jersey, USA: John Wiley & Sons, Inc, 2005.
- [19] J. W. Grizzle and E. R. Westervelt, "Hybrid zero dynamics of planar bipedal walking," *Analysis and Design of Nonlinear Control Systems*, Springer, Ed., A. Astolfi and L. Marconi, pp. 223–237, 2008.
- [20] S. W. Lipfert, *Kinematic and dynamic similarities between walking and running*. Verlag Dr. Kovač, 2010.
- [21] E. R. Westervelt, J. Grizzle, and D. E. Koditschek, "Hybrid zero dynamics of planar biped walkers," *IEEE Transactions on Automatic Control*, vol. 48, pp. 42–56, 2003.
- [22] J. Grizzle, G. Abba, and F. Plestan, "Asymptotically stable walking for biped robots: Analysis via systems with impulse effects," *IEEE Transactions on Automatic Control*, vol. 46, pp. 51–64, 2001.
- [23] J. W. Grizzle, J. Hurst, B. Morris, H. won Park, and K. Sreenath, "Mabel, a new robotic bipedal walker and runner," in *In Proc. of American Control Conference*, 2009, pp. 2030–2036.
- [24] J. W. Grizzle, C. Chevallereau, and C. long Shih, "HZD-based control of a five-link underactuated 3d bipedal robot," in *47th IEEE Conference on Decision*, 2008, pp. 5206–5213.
- [25] C. Shih, J. W. Grizzle, and C. Chevallereau, "Asymptotically stable walking of a simple underactuated 3d bipedal robot," in *In Reprint 33rd Annual Conference of IEEE Industrial Electronics (IECON 2007)*, 2007, pp. 1404–1409.
- [26] M. A. Sharbafi and A. Seyfarth, "Stable running by leg force-modulated hip stiffness," in *IEEE International Conference on Biomedical Robotics and Biomechanics (BioRob)*, 2014.